

Deep Generative Attacks and Countermeasures for Data-Driven Offline Signature Verification

An Ngo
Bucknell University
Lewisburg, Pennsylvania, USA
axn001@bucknell.edu

MinhPhuong Cao
Bucknell University
Lewisburg, Pennsylvania, USA
mtc013@bucknell.edu

Rajesh Kumar
Bucknell University
Lewisburg, Pennsylvania, USA
rk042@bucknell.edu

ABSTRACT

While previous studies have explored attacks via random, simple, and skilled forgeries, generative attacks have received limited attention in the data-driven signature verification (DASV) process. Thus, this paper explores the impact of generative attacks on DASV and proposes practical and interpretable countermeasures. We investigate the power of two prominent Deep Generative Models (DGMs), Variational Auto-encoders (VAE) and Conditional Generative Adversarial Networks (CGAN), on their ability to generate signatures that would successfully deceive DASV. Additionally, we evaluate the quality of generated images using the Structural Similarity Index measure (SSIM) and use the same to explain the attack's success. Finally, we propose countermeasures that effectively reduce the impact of deep generative attacks on DASV.

We first generated six synthetic datasets from three benchmark offline-signature datasets viz. CEDAR, BHSig260-Bengali, and BHSig260 -Hindi using VAE and CGAN. Then, we built baseline DASVs using Xception, ResNet152V2, and DenseNet201. These DASVs achieved average (over the three datasets) False Accept Rates (FARs) of 2.55%, 3.17%, and 1.06%, respectively. Then, we attacked these baselines using the synthetic datasets. The VAE-generated signatures increased average FARs to 10.4%, 10.1%, and 7.5% while CGAN-generated signatures to 32.5%, 30% and 26.1%. The variation in the effectiveness of attack for VAE and CGAN was investigated further and explained by a strong ($\rho = -0.86$) negative correlation between FARs and SSIMs. We created another set of synthetic datasets and used the same to retrain the DASVs. The retained baseline showed significant robustness to random, skilled, and generative attacks as the FARs shrank to less than 1% on average. The findings underscore the importance of studying generative attacks and potential countermeasures for DASV.

KEYWORDS

Signature verification, Deep generative models, attacks, generative attack explainability, data-driven verification system

1 INTRODUCTION

Signatures are a universally acknowledged method of identity verification, extensively utilized in diverse scenarios, including legal documents, financial transactions, workplace documentation,

governmental forms, business agreements, medical consents, intellectual property rights, and electronic documents and transactions [8, 13, 18]. In the face of escalating sophistication in contemporary scams, manual verification of human signatures is infeasible. As a result, researchers have developed strategies to automate signature verification by employing machine learning approaches [18]. Hidden Markov Models, Support Vector Machines, Neural Networks, k-nearest Neighbors, and Ensemble methods are the most widely used classifiers, achieving average error rates between 3.73 to 26.73% [16, 18].

Contemporary studies on automatic signature verification (ASV) emphasize data-driven methodologies for automation. For example, Hafemann et al. [15] employed Convolutional Neural Networks (CNN) to facilitate automated feature extraction. CNN-based techniques have outperformed the majority of statistical and traditional machine learning-based methods [18, 25, 40], obtaining superior error rates in recent investigations while exhibiting generalizability and scalability across larger and multiple datasets [9, 15]. Prior studies have examined two paradigms, namely, writer-dependent and writer-independent [16]. In this study, we experiment with a writer-dependent scenario common in the literature [16]. In other words, we train distinct models for each user. Based on the acquisition method, one can also categorize ASVs into online (dynamic) and offline (static). While only signature images are used in offline ASVs, online ASVs utilize a time-sequenced series of pen positions, pen pressure, and inclination among other [8, 13, 16, 18]. This paper focuses on offline data-driven ASVs exclusively and leaves the investigation of rest, including online ASVs, for the future.

Like other biometric systems, ASVs are susceptible to various attacks [13]. The latest survey [13] categorizes the attacks based on the impostor types as random (zero-effort or accidental) and skilled forgeries. Under random forgery, no information about the target is known to the attacker. Under skilled forgeries, the attackers have some information about the target and signature and undergo certain training. The categorization is in line with [4] classifies the forgeries into *random*, *simple*, *simulated*, and *skilled* forgeries [4]. *Random* forgery entails any signature unrelated to the genuine signer. In contrast, *simple* forgery refers to instances where the forger possesses limited knowledge of the target, such as the individual's name. *Simulated* forgery encompasses scenarios in which an inexperienced forger attempts to replicate a given signature, and *skilled* forgery involves experienced forgers practicing and perfecting their imitation of a particular signature.

Ballard et al. [1] proposed naive, trained, and generative attack classifications. They recommended generative attacks to test the robustness of ASV-like security systems, emphasizing on the effort

This work is licensed under the Creative Commons Attribution 4.0 International License. To view a copy of this license visit <https://creativecommons.org/licenses/by/4.0/> or send a



letter to Creative Commons, PO Box 1866, Mountain View, CA 94042, USA.

Proceedings on Privacy Enhancing Technologies YYYY(X), 1–10

© YYYY Copyright held by the owner/author(s).

<https://doi.org/XXXXXXXX.XXXXXXX>

required to acquire a sufficiently large number of forged samples from real participants. Readers can find the signature generation scenarios and methods taxonomy in [25]. Researchers have also explored online to offline and vice-versa signature generation [10, 25, 34]. The synthetic offline signature generation has been investigated in the past [5, 12, 25]. However, the power of generative methods such as GANs [14] and VAEs [23] is under-explored.

Therefore, we investigate the use of contemporary DGMs in attacking ASV systems and also utilize them to develop effective and interpretable countermeasures. Our main contribution is summarized below:

- Utilized two DGMs - VAE [23] and Conditional GAN [26] to generate six new synthetic datasets from forgery signatures of three public datasets, namely CEDAR [22], BHSig260-B [28] and BHSig260-H [28] for generative attack evaluation and further developments. Structural Similarity Index Measure (SSIM) [36] is used to assess the quality of the generated datasets (details in Section 3.2).
- Evaluated the robustness of three powerful deep learning architectures, viz., DenseNet201 [21], ResNet152V2 [19], and Xception [6] for automated signature verification, against different attack scenarios (details in Section 3.3 and 4.1.)
- Identified a relationship between the proximities of generated to the real images (measured by SSIM) and the success of attacks, assessed by FAR (details in Section 4.2).
- Enhanced baselines' performances with new training process utilizing SSIM-tuned generative datasets and including synthetic datasets as forgeries (details in Section 3.6 and 4.3).

The remainder of the paper is structured as follows. Section 2 reviews related studies. Section 3 details the experimental design. Section 4 presents results, analyses, and discussion. Finally, Section 5 concludes the paper and outlines future research directions.

2 RELATED WORK

2.1 Deep CNN-based offline signature verification

Hafemann et al. [15] proposed an end-to-end approach employing deep convolutional neural networks for learning features directly from offline signature images. The researchers incorporated a Siamese architecture and an innovative data augmentation technique, significantly improving performance and yielding state-of-the-art results on various benchmark datasets. Dey et al. [7] presented an architecture utilizing a Convolutional Siamese network, achieving superior error rates compared to [15] on the CEDAR dataset. Ideas from the Inception architecture (GoogLeNet) were also applied in [31]. A study by Atharva et al. [30] demonstrated the effectiveness of VGG16 for signature verification tasks. Furthermore, Yapıcı et al. [37] successfully employed VGG16, VGG19, ResNet50, and DenseNet121 architectures and implemented Cycle-GAN for data augmentation purposes. Maergner et al. [38] applied CNN using the triplet loss function and adopted ResNet-18 and DenseNet-121. Meanwhile, Chollet successfully introduced an improved version of Inception, named Xception [6], more efficiently using the previous parameters. Our baselines closely mirrored the results of those studies on the same datasets and models.

2.2 Synthetic signature generation

Synthetic signature generation has been studied for over a decade [5, 11, 12, 25]. For instance, Ferrer et al. [11] proposed an approach to generate forgeries and signatures of new identities in 2013. In a subsequent study, Ferrer et al. [12] introduced a method that emulates the human handwriting process by partitioning it into two stages: formulating an effector-independent action plan and implementing it through the corresponding neuromuscular pathway. Diaz et al. [5] proposed a cognitive-inspired algorithm based on nonlinear and linear transformations, which simulate human spatial cognitive maps and motor system intra-personal variability during the signing process. More details on signature generation scenarios and applications are available in [5]. In 2021, Maruyama et al. [25] presented an automatic method to model the most prevalent writer variability traits in the image and feature spaces and introduced an alternative approach for evaluating the quality of generated samples by considering their feature vectors.

2.3 Adversarial attacks on (D)ASV

The recent systematic survey on machine learning-based offline signature verification revealed that adversarial examples pose a substantial threat that has received limited attention from the community [18]. Hafemann et al. [17] have identified the threats to CNN-based offline signature verifiers by supplying deceptive offline signature images as input for misclassification. Although this issue is not extensively studied in the literature and requires more attention, some studies have taken the first steps.

For example, Szegedy et al. [32] have shown that adding specially crafted input perturbations to signatures can induce misclassifications in neural network-based verification models. Li et al. [24] have noted that adversarial inputs to signatures are easily recognizable by the human eye, but experiments have shown that such attacks can still impact verification models. Bird [2] has recently considered using deep generative models, such as Conditional GAN and robotic arms, to generate synthetic forgeries of signatures. The generated signatures increased FARs of CNN baseline to 29.7% for Conditional GAN and 24% and 32% with Line-us and iDraw 2.0 robots, respectively. The study concluded that using these two approaches to attack wholly human-trained systems is relatively easy. It has suggested introducing examples of such synthetic forgeries to the verification system to reduce the issue.

Tolosana et al. [33] used sequence-to-sequence VAEs for the online synthesis of short-time handwriting segments. They did not evaluate whether the generated signature would threaten ASVs and, if so, what would possibly counter the successful attacks. We conclude that the studies on deep generative attacks to *offline* signature verification are limited.

Inspired by these gaps, our research dives deeper into the usage of two generative models - CGAN and VAE (one Generative Adversarial Network and one Auto Encoder) for attacking three baseline models - Xception, DenseNet201, and ResNet152V2 across three signature datasets (CEDAR, BHSig260-B, and BHSig260-H). We also controlled the quality of synthetic signatures using SSIM, explaining why the generative attacks work and how they can be countered. More details are provided in Section 3.2.2.

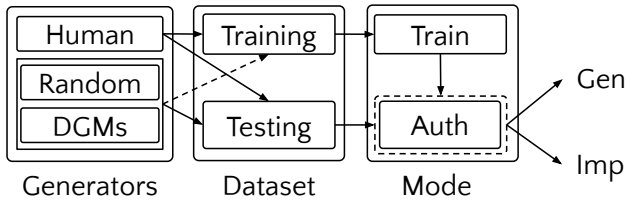


Figure 1: Overview of experiment setup. Human training and testing datasets are the signatures to generate synthetic datasets. Baseline DASVs were trained using the human training dataset and tested using and human testing dataset. Random and synthetic datasets (generated from human testing data) were used to attack the baselines. Afterward, generated datasets from human training sets were used to retrain the baselines. Finally, the retrained models were tested using human testing, random, and generated datasets from human testing. The solid arrows represent the baseline training process, and the dashed arrows indicate the retraining process.

3 DESIGN OF EXPERIMENTS

Figure 1 provides an overview of the experimental setup. The components and corresponding sub-components are described in the subsequent paragraphs.

3.1 Public datasets

We experimented with three publicly available datasets, namely CEDAR, Bengali, and Hindi, which include genuine (HumanGenuine) and forgery (HumanForged) signatures, to examine the baselines’ performances and generate synthetic datasets. All the forgery signatures provided in the listed datasets were skilled forgeries, which were made by showing a genuine signature to an individual to train and mimic. We used two-thirds of the data for training the models and the rest for testing. The entire forged datasets will also generate synthetic signatures, with the procedure described in Section 3.2.

The datasets used in this study are briefly described below:

3.1.1 CEDAR dataset. CEDAR is one of the most widely used datasets in the offline ASV domain [22]. It includes 24 genuine and 24 forged signatures for each of the 55 users, totaling 1320 genuine and as many forged signatures. Each signature is 300 dpi gray-scale and was binarized using a gray-scale histogram. Salt pepper noise removal and slant normalization were also applied to pre-process the signature images.

3.1.2 BHSig260 - Bengali dataset. The Bengali dataset consists of 100 sets of handwritten offline signatures. Each set comprises 24 genuine and 30 skilled forgeries. All signatures were collected using a Flatbed scanner with a resolution of 300DPI in gray-scale and stored in TIFF format. A histogram-based threshold was applied for binarization to convert data to two-tone images. The Bengali script has more curved shapes compared to Hindi Devanagari. It also includes unique nasal consonants and sibilants not found in Hindi, while vowel forms have a horizontal orientation.

3.1.3 BHSig260 - Hindi dataset. The Hindi dataset consists of 160 sets of handwritten offline signatures. The components and acquisition of each set are the same as the BHSig260 - Bengali dataset in Section 3.1.2. The angular Devanagari script is used for Hindi signatures. It contains distinct consonant clusters that are absent in Bengali. The Hindi vowel shapes have a more diagonal and vertical orientation than Bengali. While both datasets contain Indian script signatures, the writing styles differ due to variations in the Bengali and Hindi character sets.

3.2 Synthetic dataset generation

3.2.1 Random signature datasets. After applying the Otsu pre-processing technique and normalizing, specified in the next subsection, our original datasets are transformed into a binary array of size 224x224. Thus, to create a random attack to our baselines, we generate a dataset of 224x224 array with randomly selected values of either 0 or one. This will serve as a Random Attack to evaluate the models’ vulnerability.

3.2.2 DGM-assisted signature datasets. Among available options [3], we utilized two deep data-driven generative models, including VAE [33] and CGAN [26], to create six synthetic datasets from forgeries of each public dataset. We used CGAN and VAE because previous studies [2] have [33] successfully used it in the signature domain. Our method of generating is different from Bird et al. [2] - they supplied conditional GANs with multiple images with labels "genuine" and "forgery" and generated GAN-based images. In our study, we trained individual models for each generative architecture for each image and then generated nine synthetic samples for every original image. To avoid data leakage, images generated from the original ones classified as training sets would also be used for retraining. In contrast, ones generated from the original testing set were used for performance evaluation during attack scenarios. Each generative model is specified below:

- Conditional Generative Adversarial Networks (CGAN) is an extension of the vanilla GAN [14]. It comprises two components: a generator and a discriminator. The generator creates synthetic data samples, while the discriminator tries to distinguish between real and generated data. The key difference in CGAN is the introduction of additional conditional variables, such as labels or tags, to both the generator and the discriminator. This conditional information provides control over the types of data the generator creates. For this study, CGANs were trained on the existing datasets to create synthetic forgeries of each public dataset. Mathematically, the objective function of a CGAN is expressed as:

$$\min_G \max_D V(D, G) =$$

$$\mathbb{E}[\log D(x|y)] + \mathbb{E}[\log(1 - D(G(z|y)))]$$

- Variational Autoencoders (VAE) is a generative model that consists of two main parts: an encoder and a decoder. The encoder’s role is to compress the input data, in this case images, into a lower-dimensional latent space, while the decoder’s role is to reconstruct the original data from these compressed representations. VAEs use a variational inference approach, introducing a probabilistic layer that models the

latent space as a distribution, typically Gaussian, rather than deterministic values. In this study, VAEs were trained on images from the three human forgery datasets. The encoder was designed to map signature images to a lower-dimensional latent space, capturing the signature’s essential features and variations. On the other hand, the decoder was trained to generate signature images from the latent representations. Mathematically, VAE optimizes a different objective function, including a reconstruction loss and a regularization term. The objective function of VAE is expressed as

$$\mathcal{L}(\theta, \phi; x) = -\mathbb{E}[\log p_{\theta}(x|z)] + \text{KL}(q_{\phi}(z|x)||p(z))$$

Here, x represents input data, which is human forgeries, z is a sample from the latent space, q_{θ} is the encoder, p_{θ} is the decoder and KL represents the Kullback-Leibler divergence.

The main difference between CGAN and VAE lies in their structure and output. CGAN generates data conditioned on certain variables, giving control over the types of data the network generates. On the other hand, VAE models a low-dimensional latent space and generates data by sampling from this space. The CGAN model is adversarial, pitting two networks against each other to improve the generation process. At the same time, VAE uses an encoder-decoder structure with a probabilistic twist, introducing a distribution over the latent space. This makes it more suitable for tasks where understanding the data distribution is crucial.

3.2.3 Quality assessment of generated datasets. The quality of the generated datasets is evaluated visually through resulting images and statistically using the Structural Similarity Index Measure (SSIM). SSIM was proposed by Wang et al. [36] as a full-reference image quality assessment measure. Earlier methods of comparing images were mostly based on absolute errors such as MSE (Mean Squared Error) and PSNR (Peak Signal-to-Noise Ratio). At the same time, SSIM considers both luminance (brightness) and contrast information and the structure of the pixels in the images. It then calculates three key components: luminance (l), contrast (c), and structure (s), each designed to capture specific aspects of similarity. These components are computed using mean (μ) and standard deviation (σ) values of pixel intensities within the windows. The overall SSIM score is obtained by combining these components, producing a value of -1 to 1 , where 1 indicates perfect structural similarity, 0 denotes no similarity, and negative values indicate dissimilarity. SSIM is computed as follows:

$$l(x, y) = \frac{2 \cdot \mu_x \cdot \mu_y + C_1}{\mu_x^2 + \mu_y^2 + C_1}$$

$$c(x, y) = \frac{2 \cdot \sigma_x \cdot \sigma_y + C_2}{\sigma_x^2 + \sigma_y^2 + C_2}$$

$$s(x, y) = \frac{\sigma_{xy} + C_3}{\sigma_x \cdot \sigma_y + C_3}$$

$$SSIM(x, y) = l(x, y) \cdot c(x, y) \cdot s(x, y)$$

SSIM has been used to compare generative models’ performance in various works. In one such research [27], SSIM was used to compare the proposed architecture InfraGAN with ThermalGAN and Pix2Pix. As depicted in Figure 4, the images synthesized by VAEs exhibited the highest fidelity to the original ones, surpassing the quality of

images generated by CGANs, which exhibited diminished visual quality with excessive noise. The SSIM suggested the same results, with VAE-generated datasets achieving the highest average score of 0.8 over three datasets. In contrast, the SSIM of CGAN-generated datasets only reached 0.11. Details are presented and discussed in Table 1.

3.2.4 DGM-assisted and SSIM-controlled datasets. While creating the DGM-assisted datasets, we used a fixed number of epochs (800) to generate the synthetic datasets. That generation strategy resulted in the SSIMs reported in Table 1. We can see that with 800 epochs, VAE achieved average SSIM of 0.942, 0.510, and 0.938 for Bengali, CEDAR, and Hindi datasets, respectively. While with the same epochs, CGAN achieved average SSIM of 0.104, 0.126, and 0.108 for Bengali, CEDAR, and Hindi datasets, respectively. There was a drastic difference between the damages (FARs) done by the VAE-assisted and CGAN-assisted signatures (see Figure 6). The observation led us to investigate further how SSIM relates to FARs. We generated a range of datasets and computed a correlation between the FARs achieved by those datasets and the respective SSIMs. The relationship (strong negative correlation) between the SSIM and FARs was uncovered and demonstrated in Figure 2.

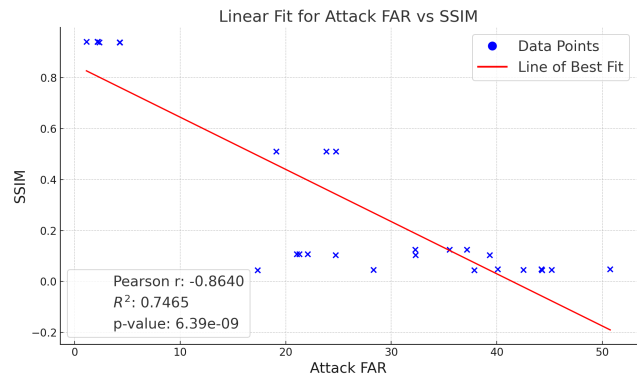


Figure 2: A deeper investigation into how the quality of images measured by SSIM impacts the attack success (FARs) revealed a strong negative correlation between SSIM and FARs. The observation motivated us to build a novel countermeasure, i.e., retraining the models using SSIM-controlled datasets.

The uncovered relationship between SSIM and FARs led us to generate an SSIM-controlled dataset for attack and countermeasures. Because attackers can always arrange impostor signature samples, we kept the data generation process centered around impostor samples. In other words, we used impostor samples as the reference for data generation via DGMs. The goal was to generate signatures away from the impostor samples so the generated samples could be misclassified as genuine, increasing the FARs. In other words, we wanted to generate signature samples from impostor samples with the lowest SSIM.

We generated 5 signatures per user from the impostor samples at different numbers of epochs and plotted the same to realize that the CGAN could only generate signatures with very low SSIM. At

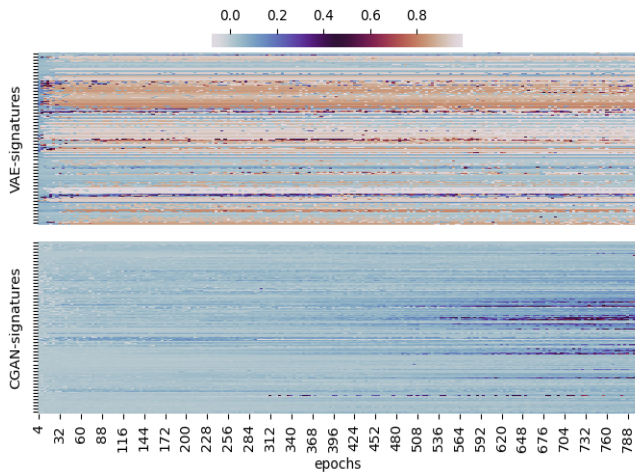


Figure 3: Comparison of the distribution of SSIM achieved by CGAN and VAE-based signature generators. We can see the power of each generator over different epochs studied in this paper without tuning them using SSIMs. On the y-axis, we have 275 signature samples generated by respective generators, five samples per user, and the map’s heat indicates the SSIMs of each signature. VAE could generate signatures close to reference signatures (skilled forgeries) across varying epochs. At the same time, CGAN could not do so even with a significantly high number of epochs.

the same time, VAE could generate either very high SSIM or very low SSIMs (see Table 1).

Table 1: Initial experiments suggested that CGAN consistently generated low SSIM (away from the reference image) images compared to the VAE, which was able to generate images with high SSIMs. We were required to generate signatures with low SSIM to retrain the models as the FAR was negatively correlated with SSIMs. Hence, VAE was selected over CGAN to generate the signatures, later used for retraining the authentication models.

Dataset	VAE SSIM	CGAN SSIM	VAE SSI-tuned SSIM
Bengali	0.942	0.104	0.048
CEDAR	0.510	0.126	0.045
Hindi	0.938	0.108	0.045

Considering the ability of VAE to generate signatures in a wide range of spectrum of SSIM (see Figure 3), we decided to use VAE to generate images with the lowest possible SSIM. We generated signatures with SSIM less than 0.05 for attacking the baselines and testing the SSIM-controlled countermeasure (see Table 1).

The VAE models were retrained with the same dataset until the generated signatures reached the SSIM that could be considered insignificant. In particular, instead of training our deep-learning

baselines with a fixed number of 800 epochs and using the final generator to generate signatures, we sample one signature per 5 epochs during the training. If the signatures are within the threshold (in this case, we choose 0.04 – 0.08), we stop the training and keep the sampled signature. If after 800 epochs, no signature was kept, the model is retrained from the beginning. The process is repeated 9 times for each signature to get 9 generated samples, similar to the uncontrolled dataset. We name this dataset as VAE-SSI-Controlled dataset.

The new VAE-SSI-Controlled dataset further confirmed our observation of a negative correlation between SSIM and FAR, as the VAE-SSI-Controlled dataset achieved higher FARs than the epoch-guided ones. The epoch-guided dataset is referred to as the VAE dataset, while SSI controlled dataset will be referred to as VAE-SSI-Controlled hereafter.

3.3 Deep signature verification baselines

3.3.1 Baseline Models. The three Deep Convolutional Neural Network models - Xception, ResNet152V2, and DenseNet201 would be used as feature extractors to train user-specific signature authentication models. Each user will have a personal model trained with their signature set only for each model type. Evaluation of the models across all users is provided in the subsequent sections.

3.3.2 Data Preprocessing & Vanilla Training Process. We first applied the Otsu method for image pre-processing on the three datasets mentioned above. Subsequently, the images are resized to 224x224 using the bi-cubic interpolation method, and they are normalized before being put into the feature extractors. The same pre-processing technique is also applied during testing/attacking. We trained individual models for each user in our datasets using the first two-thirds of their genuine and forged signatures. The remaining one-third of each user’s dataset, consisting of synthetic signatures generated from their genuine and forged signatures, was used for testing. The authentication model consists of a simple dense layer with 256 nodes with activation function *ReLU*. Finally, we have another dense layer with two nodes representing the output layer with genuine and impostor signatures. These layers use the Sigmoid activation function. Since this was a classification problem, we used binary cross-entropy with a Stochastic Gradient Descent (SGD) optimizer and a learning rate 0.0001 with momentum as 0.9.

The resulting models from this training process are called Vanilla Baselines to distinguish from systems retrained with our proposed approach.

3.4 Threat model

This paper considers a different threat model from the one investigated in [17]. In [17], Hafemann et al. investigated the adversarial methods: Carlini, Fast Gradient Method, and Simulated annealing, all requiring full knowledge of the model - the white box scenario. This paper considers the black box-injection attacking scenario similar to the one presented in [39] for deceiving gait, touch, face, and voice-based verification. The attackers cannot access the full verification model in this kind of attack. However, the attackers need access to the samples the verifiers accept. One can obtain the legitimate sample by stealing or using the membership inference idea presented in [29].

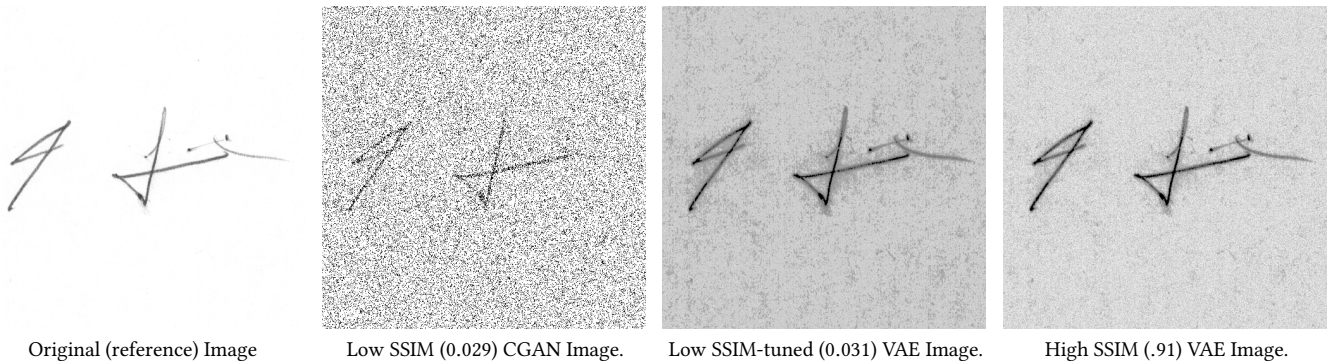


Figure 4: Illustrating the original (reference for DGMs) signatures and the corresponding generated signatures using CGAN and VAE for different SSIMs i.e., with controlled and uncontrolled generation. The second and third images demo low-quality generated signatures (with SSIMs about 0.03) by CGAN and VAE SSI-tuned. While the last generated signature shows high-quality images with SSIM as high as 0.9.

3.5 The attack scenarios

We use four attack scenarios to assess the baseline models' attack susceptibility to attacks. The impacts of each attack were calculated using False Accept Rates (FARs). The higher the FARs are, the more successful the attack

3.5.1 Vanilla Attack. Vanilla Attack revolved around traditional impostor testing with the HumanForge dataset from the three public datasets: CEDAR, BHSig260 - Bengali, and Hindi. This attack is the primary attack scenario used to evaluate baseline performance, facilitate comparison with previous studies, and highlight the performance of various other attacks.

3.5.2 Random Attack. We adopted this attack from [39], which studied random vector attacks for deceiving gait, touch, face, and voice-based verification. Following the suit, we generated 5000 random images to attack and evaluate each baseline.

3.5.3 VAE and CGAN Attack. In this attack scenario, we used VAE-generated signatures to test if they could bypass the signature verification process. In contrast to VAE-generated signatures, CGAN-generated signatures had more significant disparities from the reference images. We hypothesized and expected CGAN-generated signatures to produce a higher FAR because the generated images were away from the impostor images, resulting in a higher chance of being classified as genuine. This hypothesis was further investigated by exploring if there was a relationship between SSIM and FARs.

3.6 Countermeasures

3.6.1 Retraining with synthetic datasets as impostors. We propose synthetic data augmented retraining of DASVs to increase their robustness to the studied attacks. First, we retrain each DASV, considering random and DGM-assisted datasets and human forgeries as impostor samples. The re-training process resulted in three new models, namely random-assisted, VAE-assisted, and CGAN-assisted models. We then tested the retrained models using the same attack scenarios and evaluation metrics.

For random-assisted systems, the random dataset used to train was created in isolation, ensuring the separation from the random images used in the retraining process. For synthetic datasets, as mentioned above, the VAE dataset and CGAN dataset were split into training and testing sets. In this retraining process, we used the training portion to retrain our baselines, which resulted in VAE-assisted and CGAN-assisted models. Assisted models were then tested on synthetic images originating from testing datasets. This was done to ensure the testing set remains unseen to our retrained models. We expected that this retraining process would accommodate our systems with more unfamiliar territories and, thus, improve their performances in unobserved contexts.

3.6.2 SSIM-tuning. While evaluating the baseline authentication models under GAN-assisted attack scenarios, we identified a strong negative correlation between the SSIM of generated images and FAR (specified in Section 4.2). In other words, the lower the SSIM is, the higher the FAR. Thus, models trained with low SSIM signatures were expected to be more robust to different attack scenarios.

This observation led to our design of and enhancing retraining techniques to our baseline. Since the original VAE dataset's performance is not high, we applied SSIM to fine-tune this DGM. In this process, we retrain our VAE models with the same dataset settings until the generated images reach the SSIM that could be considered insignificant. In particular, instead of training our deep-learning baselines with a fixed number of 800 epochs and using the final generator to generate images, we sample one image per 5 epochs during the training. If the image is within the threshold (in this case, we choose 0.04 – 0.08), we stop the training and keep the sampled image. If no image is kept after 800 epochs, the model will be retrained from the beginning. The process is repeated 9 times each signature image to get 9 generated samples, similar to the uncontrolled dataset.

The new VAE SSI dataset further confirms our observation of a negative correlation between SSIM and FAR. The new VAE SSI dataset also poses a greater threat to the baseline than the VAE dataset before, and it would be used to test or retrain the retrained

models. In this paper, we will call the VAE SSI-tuned dataset VAE SSI to differentiate between the initial VAE dataset.

3.7 Performance Evaluation

The performance of the baseline models was assessed under two distinct conditions—the first was to evaluate the models’ proficiency in accepting genuine signatures, and the second was to reject non-genuine signatures. The performance was quantified using False Reject Rates (FRR), probabilistically complementary to True Accept Rates (TAR). In contrast, the models’ capability to reject non-genuine signatures was quantified by False Accept Rates (FAR), probabilistically complementary to True Reject Rates (TRR), measured from four different attack scenarios listed above. The Half Total Error Rate (HTER), which is the average of FAR and FRR, is also reported for comparison convenience.

4 RESULTS & DISCUSSION

4.1 Baseline Performance

Figure 5 presents the performance of the three baseline models, namely Xception, ResNet152V2, and DenseNet201, across three different CEDAR, BHSig260 - Bengali, and Hindi datasets. We can observe that all three models consistently achieved low error rates of under 6% in both FAR and FRR, verifying the performance of selected models for further investigation. We can observe that DenseNet201 is the top performer in Signature Verification with the HTER of 1.81%, followed by Xception (3.52%) and ResNet152V2 (4.43%) from the CEDAR dataset. With BHSig260 datasets, while DenseNet201 obtained the lowest HTER, we observed a slightly better performance for ResNet152V2 than Xception. For BHSig260 - Bengali, DenseNet201 achieved HTER of 0.44%, followed by ResNet152V2 (1.65%) and Xception (1.652%). For BHSig260 - Hindi, DenseNet201, ResNet152V2 and Xception obtained HTER of 1.73%, 3.66% and 4.26% respectively.

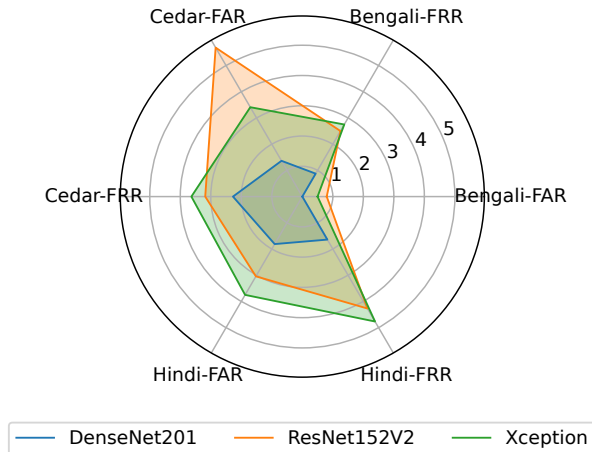


Figure 5: Baseline performance of the models. All models achieved low error rates below 6% for FAR and FRR. Although not included in the Figure, HTER was used to compare the performance (refer to Section 4.1).

This performance closely followed the results presented in [31], [37], suggesting that those three models can be a verified baseline to evaluate the attack scenarios conducted using datasets generated from VAE and CGAN that will be discussed in later sessions.

4.2 Attack Performance

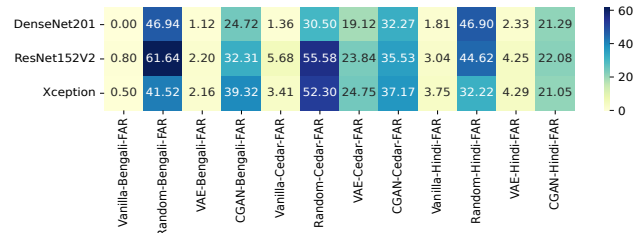


Figure 6: Attack performance on the baseline performance of the models. It is important to note that the synthetic signatures were generated using skilled forgeries as a reference, and each DGM ran for 800 epochs. The higher the SSIM, the more similar the generated signature is to the forgeries, in turn, the lower the FAR. In contrast, the lower the SIM is, the farther the generated signature is from the reference forgeries, in turn, the higher the FAR. Random attacks resulted in high vulnerability with FAR over 30% on average. VAE attacks produced FAR closest to original forgeries, except for CEDAR models, which had higher FAR of around 20-25%. CGAN attacks caused the highest FAR, exceeding 29% on average across all models and datasets.

The effect of described attack scenarios is presented in Figure 6 measured using FAR.

4.2.1 *Random Attacks.* Figure 6 reveals that although our baseline systems exhibited low FARs against skilled forgeries, they were highly vulnerable to even random attacks across all three models. In particular, ResNet152V2 trained on the Bengali dataset appears to have the highest FAR on random attacks. Similarly, on average, other models’ FAR on random attacks reached higher than 30.5%.

4.2.2 *CGAN Attacks.* The baseline attack results also reveal that despite previously indicating that CGAN-generated images had great disparities from the original datasets, CGAN datasets appear to have significant impacts when used as attacks to our baseline models. In particular, the CGAN-generated dataset produced a much higher FAR than VAE’s, with an average of 29.5 % across all three models trained on three datasets. This error rate also far exceeded original Human Forgeries. The reason is that the CGAN-generated signatures were far from skilled forgeries, in turn, close to genuine signatures, resulting in higher FARs. In contrast, the VAE-generated signatures were closer to the human forgeries, resulting in rejections by the DASVs, causing lower FARs than CGAN generated images.

4.2.3 *VAE Attacks.* Presented in Figure 6, the attack’s results using VAE datasets closely mirrored our anticipated outcomes. We observed that most of the results from VAE Forg2Syn came close

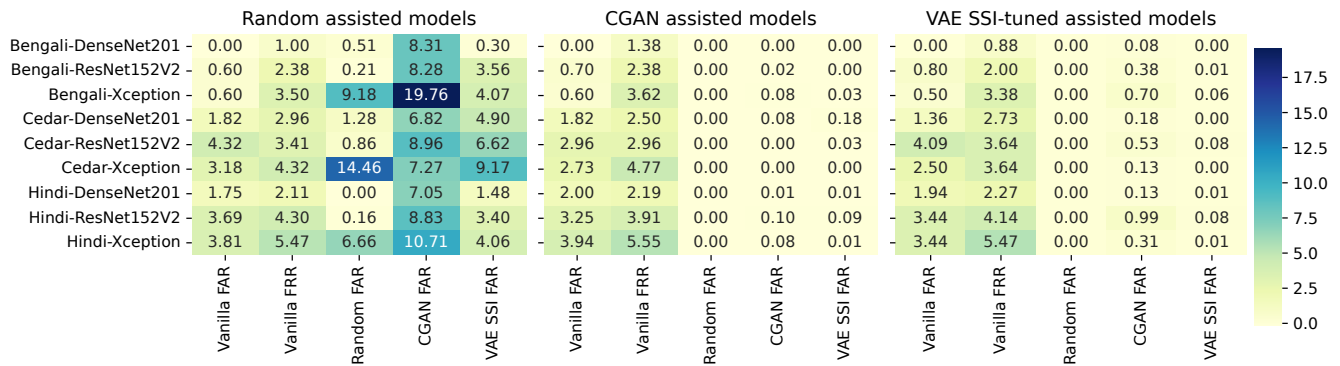


Figure 7: Heatmaps showing the performance of retrained models in the presence of various adversaries. The x-axis labels indicate the type of attacks, and the y-axis labels denote the combination of the dataset and underlying deep learning architecture used to train the authentication models. The heatmap values in each cell indicate the false accept rate for the corresponding combination of rows and columns and the retraining method. The first heatmap (from the left) is for the models that were retrained using the random signature images. Likewise, the second and third heatmaps correspond to the models that were retrained using the CGAN-generated signatures and VAE-SSI tuned-generated signatures. We can see that the CGAN and VAE-SSI-based retraining pushes the FARs below 1%, showing our proposed approach’s superiority over vanilla or the random signature-assisted training processes. The Random, CGAN, and VAE-SSI attacks impact only the FARs, so we are reporting only FARs for them, while in the Vanilla attack scenario, we retested the retrained models for both genuine and impostor pass/fail; hence, there is Vanilla FAR and Vanilla FRR. If we compare the Vanilla FRR in these heatmaps with the FRRs presented in Figure 5, we can see that the retrained models maintain the FRR of the initial models. The retrained models beat or closely matched the initial models while defending from adversaries, i.e., significantly reducing the FARs.

to the original forgery samples across all datasets, with the slight exception of those trained on CEDAR. In particular, DenseNet201, ResNet152V2, and Xception trained on Vanilla Bengali have FARs according to Vanilla attacks of 0%, 0.8% and 0.5% compared to the FARs on VAE attacks of 1.12%, 2.20% and 2.16% respectively. Likewise, for the three models trained on Vanilla Hindi, the FARs of Vanilla attacks are 1.36%, 5.68% and 3.41% in comparison to the FARs of VAE attacks of 2.33%, 4.25% and 4.29%. CEDAR-trained models were more affected by this type of attack, evident in the considerably higher FAR of 19.12%, 23.84%, and 24.75% resulting from the VAE attacks.

4.3 Retrained Baselines Performance

4.3.1 Random-assisted models. The first heatmap in Figure 7 suggests that while the FAR and FRR tested on Human Genuine and Human Forgeries experienced slight changes, random-assisted models demonstrated higher robustness to random and generated datasets (compare the FARs in Figure 6 and Figure 7). However, the FARs of Random assisted models remained high under Random, CGAN, and VAE attacks for most of the datasets and model combinations.

4.3.2 CGAN-assisted models. The second heatmap in Figure 7 suggests that the CGAN-assisted models showed very high robustness against each attack. In particular, the FAR for all random attacks has been minimized to 0% and CGAN attacks under 0.10%, followed by the Vanilla attack under 0.18% in the worst case.

4.3.3 VAE-assisted models. The third heatmap (from the left) shown in Figure 7, suggests that the VAE-assisted retraining drastically improved the robustness of the models under all the attacks. In

particular, VAE-assisted models also obtained 0% FAR on random attack. The models also show significant improvements in CGAN attacks, despite not as much as CGAN-assisted models, and VAE-SSI attacks. Particularly, the FAR falls in the range of 0.08 - 0.99% for CGAN attacks and 0.0-0.08% for VAE-SSI attacks. The models’ FAR on VAE-SSI attacks was slightly lower, with an average of 0.026%, compared to 0.038% for CGAN-assisted models.

4.4 Implications

This research reveals vulnerabilities in data-driven automated signature verification (DASV) systems to synthetic forgery attacks using deep generative models (DGMs). By generating fake but realistic-looking forged signatures, DGMs can severely degrade DASV performance, indicated by alarmingly high false acceptance rates. This highlights the inability of current DASV models to detect state-of-the-art generative forgeries adequately.

We propose an enhanced training methodology incorporating DGM-produced synthetic forgeries to address this weakness. We used structural similarity tuning to generate samples and used that samples to maximized training impact. This improved model robustness, demonstrating the value of adversarial generative training.

These findings point to necessary improvements in applying DASV for real-world authentication in sectors like finance and banking. New safeguards are needed to protect against DGM signature attacks, such as forensic techniques to identify generative artifacts. Hardening DASV models through adversarial training and developing architectures better suited for signature analysis can create more attack-resistant systems.

By revealing current vulnerabilities, this research paves the way for the next generation of DASV technologies ready for reliable deployment. Developing more robust models resistant to emerging generative threats will enable the widespread adoption of data-driven automatic signature verification in authentication workflows. With vigilance and ongoing innovation, DASV can overcome this challenge to securely authenticate identities in key applications.

We anticipate similar vulnerability exists in several other architectures that have been studied for ASV and aim to study them in the future. In addition, we anticipate that other behavioral biometrics are also prone to such attacks and plan to look into walking, typing, voice and swiping-based authentication systems.

4.5 Conclusion & Future Work

In this study, we examined the vulnerability of DASV systems to attack scenarios, namely Vanilla, Random, VAE, and CGAN attacks, to data-driven signature verification systems. Next, we established a relationship between generation quality and FAR. Finally, we proposed new DASVs that are robust to generative attacks.

The results indicated that Vanilla models, trained on traditional processes, only showed good performances on Vanilla attacks while having notably high vulnerability to random and generative attacks. This discovery inspired us to retrain the systems with random and generated datasets to improve their robustness. The results also led us to observe a negative correlation between the SSIM of generative datasets and FAR, which resulted in our retraining methods with SSI tuning techniques. Our proposed methods of system retraining resulted in enhanced systems that were capable of both maintaining the robustness of Vanilla attacks and enhancing performances on random and generated attacks.

Our finding of the negative relationship between the DASV's FAR and the SSIM of the models is noteworthy and paves the way for improving the robustness of security systems. Such a finding suggests an explanation of the attack performance from Deep Generative signature by the image quality. This also suggests that SSIM-tuning signature image generation can be used to control the attacks' performance. We believe these findings can help build more robust and resilient verification models and provide more knowledge on their explainability in the future.

For our future work, we expect to investigate further the correlation between SSIM and FAR of signature verification systems and how it can be utilized more to improve the systems. In addition, we would try to investigate more image quality metrics such as the Fréchet Inception Distance [20], the Universal Image Quality index [35], and their relationship with deep generative signature attacks FAR. We would also explore how datasets generated from genuine human signatures can enhance these systems. The studies would be extended to online signatures as well.

REFERENCES

- [1] Lucas Ballard, Daniel Lopresti, and Fabian Monrose. 2007. Forgery quality and its implication for behavioural biometric security. *IEEE Trans Syst Man Cybern Part B. IEEE transactions on systems, man, and cybernetics. Part B, Cybernetics : a publication of the IEEE Systems, Man, and Cybernetics Society* 37 (11 2007), 1107–18. <https://doi.org/10.1109/TSMCB.2007.903539>
- [2] Jordan J Bird. 2022. Robotic and Generative Adversarial Attacks in Offline Writer-independent Signature Verification. *arXiv preprint arXiv:2204.07246* (2022).
- [3] Sam Bond-Taylor, Adam Leach, Yang Long, and Chris G. Willcocks. 2022. Deep Generative Modeling: A Comparative Review of VAEs, GANs, Normalizing Flows, Energy-Based and Autoregressive Models. *IEEE Transactions on Pattern Analysis and Machine Intelligence* (Nov 2022). <https://doi.org/10.1109/TPAMI.2021.3116668>
- [4] Walid Bouamra, Chawki Djeddi, Brahim Nini, Moises Diaz, and Imran Siddiqi. 2018. Towards the design of an offline signature verifier based on a small number of genuine samples for training. *Expert Systems with Applications* (2018).
- [5] Moisés Díaz Cabrera, Miguel Angel Ferrer-Ballester, George S. Eskander, and Robert Sabourin. 2017. Generation of Duplicated Off-Line Signature Images for Verification Systems. *IEEE Transactions on Pattern Analysis and Machine Intelligence* (2017).
- [6] François Chollet. 2016. Xception: Deep Learning with Depthwise Separable Convolutions. *CoRR abs/1610.02357* (2016). <http://arxiv.org/abs/1610.02357>
- [7] Sounak Dey, Anjan Dutta, J. Ignacio Toledo, Suman K. Ghosh, Josep Lladós, and Umapada Pal. 2017. SigNet: Convolutional Siamese Network for Writer Independent Offline Signature Verification. *arXiv:1707.02131 [cs.CV]*
- [8] Moises Diaz, Miguel A. Ferrer, Donato Impedovo, Muhammad Imran Malik, Giuseppe Pirlo, and Réjean Plamondon. 2019. A Perspective Analysis of Handwritten Signature Technology. *ACM Comput. Surv.* (Jan 2019).
- [9] E. Allan Farnsworth. 2019. Large-scale offline signature recognition via deep neural networks and feature embedding. *Neurocomputing* 359 (2019), 1–14. <https://doi.org/10.1016/j.neucom.2019.03.027>
- [10] M. A. Ferrer, M. Diaz, C. Carmona-Duarte, and R. Plamondon. 2020. iDeLog: Iterative Dual Spatial and Kinematic Extraction of Sigma-Lognormal Parameters. *IEEE Transactions on Pattern Analysis & Machine Intelligence* 42, 01 (jan 2020), 114–125. <https://doi.org/10.1109/TPAMI.2018.2879312>
- [11] Miguel A. Ferrer, Moises Diaz-Cabrera, and Aythami Morales. 2013. Synthetic off-line signature image generation. In *2013 International Conference on Biometrics (ICB)*. <https://doi.org/10.1109/ICB.2013.6612969>
- [12] Miguel A. Ferrer, Moises Diaz-Cabrera, and Aythami Morales. 2015. Static Signature Synthesis: A Neuromotor Inspired Approach for Biometrics. *IEEE Trans. Pattern Anal. Mach. Intell.* (mar 2015), 667–680. <https://doi.org/10.1109/TPAMI.2014.2343981>
- [13] Carlos Gonzalez-Garcia, Ruben Tolosana, Ruben Vera-Rodriguez, Julian Fierrez, and Javier Ortega-Garcia. 2023. Introduction to Presentation Attacks in Signature Biometrics and Recent Advances. *arXiv:2302.08320 [cs.CV]*
- [14] Ian J. Goodfellow, Jean Pouget-Abadie, Mehdi Mirza, Bing Xu, David Warde-Farley, Sherjil Ozair, Aaron Courville, and Yoshua Bengio. 2014. Generative Adversarial Networks. (2014). *arXiv:1406.2661 [stat.ML]*
- [15] Luiz G. Hafemann, Robert Sabourin, and Luiz S. Oliveira. 2017. Learning features for offline handwritten signature verification using deep convolutional neural networks. *Pattern Recognition* (2017).
- [16] Luiz G. Hafemann, Robert Sabourin, and Luiz S. Oliveira. 2017. Offline handwritten signature verification — Literature review. In *2017 Seventh International Conference on Image Processing Theory, Tools and Applications (IPTA)*.
- [17] Luiz G Hafemann, Robert Sabourin, and Luiz S Oliveira. 2019. Characterizing and evaluating adversarial examples for offline handwritten signature verification. *IEEE Transactions on Information Forensics and Security* 14, 8 (2019), 2153–2166.
- [18] M. Muzaffar Hameed, Rodina Ahmad, Miss Laiha Mat Kiah, and Ghulam Murtaza. 2021. Machine learning-based offline signature verification systems: A systematic review. *Signal Processing: Image Communication* (2021).
- [19] Kaiming He, Xiangyu Zhang, Shaoqing Ren, and Jian Sun. 2016. Identity Mappings in Deep Residual Networks. *arXiv:1603.05027 [cs.CV]*
- [20] Martin Heusel, Hubert Ramsauer, Thomas Unterthiner, Bernhard Nessler, and Sepp Hochreiter. 2017. Gans trained by a two time-scale update rule converge to a local nash equilibrium. *Advances in neural information processing systems* 30 (2017).
- [21] Gao Huang, Zhuang Liu, Laurens Van Der Maaten, and Kilian Q. Weinberger. 2017. Densely Connected Convolutional Networks. *2017 IEEE Conference on Computer Vision and Pattern Recognition (CVPR)* (2017), 2261–2269. <https://doi.org/10.1109/CVPR.2017.243>
- [22] Meenakshi K. Kalera, Sargur N. Srihari, and Aihua Xu. 2004. Offline Signature Verification And Identification Using Distance Statistics. *Int. J. Pattern Recognit. Artif. Intell.* 18 (2004), 1339–1360.
- [23] Diederik P Kingma and Max Welling. 2013. doi: 10.48550/ARXIV.1312.6114. Auto-Encoding Variational Bayes. *CoRR* (2013). doi: 10.48550/ARXIV.1312.6114.
- [24] Haoyang Li, Heng Li, Hansong Zhang, and Wei Yuan. 2021. Black-box attack against handwritten signature verification with region-restricted adversarial perturbations. *Pattern Recognition* 111 (2021), 107689.
- [25] Teruo M. Maruyama, Luiz S. Oliveira, Alceu S. Britto, and Robert Sabourin. 2021. Intrapersonal Parameter Optimization for Offline Handwritten Signature Augmentation. *IEEE Transactions on Information Forensics and Security* (2021).
- [26] Mehdi Mirza and Simon Osindero. 2014. Conditional Generative Adversarial Nets. <http://arxiv.org/abs/1411.1784>
- [27] Mehmet Akif Özkanoglu and Sedat Ozer. 2022. InfraGAN: A GAN Architecture to Transfer Visible Images to Infrared Domain.
- [28] Srikanta Pal, Alireza Alaei, Umapada Pal, and Michael Blumenstein. 2016. Performance of an Off-Line Signature Verification Method Based on Texture Features on a Large Indic-Script Signature Dataset. In *2016 12th IAPR Workshop on Document Analysis Systems (DAS)*, 72–77. <https://doi.org/10.1109/DAS.2016.48>

- [29] Reza Shokri, Marco Stronati, and Vitaly Shmatikov. 2016. Membership Inference Attacks against Machine Learning Models. *CoRR* abs/1610.05820 (2016).
- [30] Karen Simonyan and Andrew Zisserman. 2014. Very deep convolutional networks for large-scale image recognition. *arXiv preprint arXiv:1409.1556* (2014).
- [31] Christian Szegedy, Vincent Vanhoucke, Sergey Ioffe, Jonathon Shlens, and Zbigniew Wojna. 2015. Rethinking the Inception Architecture for Computer Vision. *CoRR* abs/1512.00567 (2015).
- [32] Christian Szegedy, Wojciech Zaremba, Ilya Sutskever, Joan Bruna, Dumitru Erhan, Ian Goodfellow, and Rob Fergus. 2014. Intriguing properties of neural networks. *International Conference on Learning Representations* (2014). <http://arxiv.org/abs/1312.6199>
- [33] Ruben Tolosana, Paula Delgado-Santos, Andres Perez-Urbe, Ruben Vera-Rodriguez, Julian Fierrez, and Aythami Morales. 2021. DeepWriteSYN: On-Line Handwriting Synthesis via Deep Short-Term Representations. In *AAAI Conf. on Artificial Intelligence (AAAI)*. <https://doi.org/abs/2009.06308>
- [34] Ruben Vera-Rodriguez, Ruben Tolosana, Javier Hernandez-Ortega, Alejandro Acien, Aythami Morales, Julian Fierrez, and Javier Ortega-Garcia. 2018. *Modeling the Complexity of Signature and Touch-Screen Biometrics using the Lognormality Principle*. https://doi.org/10.1142/9789811226830_0003
- [35] Zhou Wang and A.C. Bovik. 2002. A universal image quality index. *IEEE Signal Processing Letters* 9, 3 (2002), 81–84. <https://doi.org/10.1109/97.995823>
- [36] Zhou Wang, A.C. Bovik, H.R. Sheikh, and E.P. Simoncelli. 2004. Image quality assessment: from error visibility to structural similarity. *IEEE Transactions on Image Processing* (2004). <https://doi.org/10.1109/TIP.2003.819861>
- [37] Muhammed Mutlu Yapıcı, Adem Tekerek, and Nurettin Topaloğlu. 2021. Deep Learning-Based Data Augmentation Method and Signature Verification System for Offline Handwritten Signature. *Pattern Anal. Appl.* (2021).
- [38] Muhtar Yusnur, Wenxiong Kang, Rexit Aliya, Mahpirat, and Ubul Kurban. 2022. A Survey of Offline Handwritten Signature Verification Based on Deep Learning. <https://doi.org/10.1109/PRML56267.2022.9882188>
- [39] Benjamin Zhao, Hassan Asghar, and Mohamed Ali Kaafar. 2020. On the Resilience of Biometric Authentication Systems against Random Inputs. *Network and Distributed System Security Symposium* (2020).
- [40] Elias N. Zois, Ilias Theodorakopoulos, and George Economou. 2017. Offline Handwritten Signature Modeling and Verification Based on Archetypal Analysis. In *2017 IEEE International Conference on Computer Vision (ICCV)*. 5515–5524. <https://doi.org/10.1109/ICCV.2017.588>